journal

J. Am. Ceram. Soc., **98** [6] 1685–1697 (2015)
DOI: 10.1111/jace.13639
© 2015 The American Ceramic Society

Modeling of Probabilistic Failure of Polycrystalline Silicon MEMS Structures

Jia-Liang Le,[‡,†] Roberto Ballarini,[§] and Zhiren Zhu[¶]

[‡]Department of Civil, Environmental, and Geo- Engineering, University of Minnesota, Minneapolis, Minnesota

[§]Department of Civil and Environmental Engineering, University of Houston, Houston, Texas

[¶]Department of Civil, Environmental, and Geo- Engineering, University of Minnesota, Minneapolis, Minnesota

Microelectromechanical Systems (MEMS) devices typically need to be designed against a very low failure probability, which is on the order of 10^{-4} or lower. Experimental determination of the target strength for such a low failure probability requires testing of tens of thousands of specimens, which can be cost prohibitive for the design process. Therefore, understanding the probabilistic failure of MEMS devices is of paramount importance for design. Currently available probabilistic models for predicting the strength statistics of MEMS structures are based on classical Weibull statistics. Significant advances in experimental techniques for measuring the strength of MEMS devices have produced data that have unambiguously demonstrated that the strength distributions consistently deviate from the Weibull distribution. Such deviations can be explained by the fact that the Weibull distributions are derived based on extreme value statistics, which is inapplicable to MEMS devices where the dimensions of the material microstructure are not negligible compared to the characteristic structural dimensions. This paper presents a robust probabilistic model for strength distribution of polycrystalline silicon (poly-Si) MEMS structures that could be extended to other brittle materials at the microscale. The overall failure probability of the structure is related to the failure probability of each material element along its sidewalls through a weakest-link statistical model. The failure statistics of the material element is determined by both the intrinsic random material strength as well as the random stress field induced by the sidewall geometry. Different from the classical Weibull statistics, the present model is designed to account for structures consisting of a finite number of material elements, and it predicts a scale effect on their failure statistics. It is shown that the model agrees well with the measured strength distributions of poly-Si MEMS specimens of different sizes, and the calibrated mean strength of the material element is consistent with the theoretical strength of silicon. Meanwhile, it is shown that the two-parameter and three-parameter Weibull distributions cannot provide optimum and consistent fits of the observed size-dependent strength distributions, and thus have very limited prediction capability. The present model explicitly relates the strength statistics to the size effect on the mean structural strength, and therefore provides an efficient means of determining the failure statistics of MEMS structures.

I. Introduction

During the early development of Microelectromechanical Systems (MEMS) technology, structural reliability was not considered a critical issue because devices were subjected to relatively small fractions of the materials' stress and strain limits. These include the silicon structural components contained in the guts of Analog Devices' air bag accelerometer that are protected also from potential environment-induced material degradation by hermetic sealing. The failure of but one of 1300 of these devices when subjected to mechanical shock and a range of temperatures led to their assessment as structurally highly reliable.[1] But note that in applications that require extremely high reliability, a probability of fracture of 7.7×10^{-4} (1/1300) may not suffice. The Texas Instruments (TI) Digital Micromirror Device is another celebrated device consisting of hundreds of thousands aluminum mirrors that was tested in excess of one trillion cycles without a single failure.[2] As pointed out by Boyce et al.,[3] these successes demonstrated that MEMS devices can be implemented through good engineering practice. However, while voltage-compensated accelerometers such as those developed by Analog Devices do not operate near the strain limits, devices that are designed to operate at high mechanical power densities and/or large deformation levels will be required to do so.[4] Therefore, there has been a continuing interest in understanding the reliability of MEMS materials and structures.[4–8]

The work-horse material used to fabricate surface micromachined MEMS devices is polycrystalline silicon (poly-Si).[9,10] The fracture strength of MEMS-scale poly-Si volumes is governed by processing-induced surface defects, and less commonly defects within the volume. The stochastic distribution of surface flaws and the spatial distribution of stress lead to a wide variation in the material's nominal tensile strength; from 1 GPa in direct tension to 6 GPa in the vicinity of stress-concentrating notches.[5] In direct tension the

R. Ballarini—contributing editor

Manuscript No. 36462. Received February 25, 2015; approved April 12, 2015.
[†]Author to whom correspondence should be addressed. e-mail: jle@umn.edu

Feature

probability that all flaws including the largest are subjected to the highest stress is assured. In a notched specimen on the other hand the largest flaw may experience much lower values of stress, or alternatively the region of highest stress may contain relatively small flaws. Petersen[11] recognized that silicon structures "should have the lowest possible bulk, surface and edge crystallographic defect density to minimize potential regions of stress concentration"; but eliminating processing-induced defects is not a trivial task. Over the years, significant variability of fracture strength has also been observed in MEMS devices made of other materials such as silicon carbide, ultrananocrystalline diamond and hydrogen-free tetrahedral amorphous carbon.[6,7]

Due to the inevitable variability in fracture strength of MEMS devices, the importance of proof testing has been emphasized for reliability analysis of MEMS devices.[3] The main challenge in experimental investigation of structural reliability of MEMS devices is to due the fact that the design should target a failure probability on the order of 10^{-4} or lower.[5] Due to the limitation of mechanical testing procedures of MEMS materials, early histogram testing involved small numbers of specimens,[12–15] which could not capture the failure probability function. To facilitate more efficient histogram testing of MEMS devices, a slack-chain tester was recently developed at the Sandia National Laboratories that allows sequential tension tests on a large number of specimens (~ 1000 specimens) in a short time.[8] Nevertheless, the existing experimental approaches are still hampered by two difficulties: (1) it is cost prohibitive to experimentally determine the strength corresponding to a low failure probability (e.g. $P_f \approx 10^{-4}$), which is often required in the design; and (2) it is unfeasible to perform histogram testing for MEMS devices of various kinds of geometries since most experimental platforms are designed for specific types of specimen geometries and loading configurations. Therefore, fundamental understanding of the probabilistic failure of MEMS devices subjected to high levels of and/or different types of mechanical forces is of paramount importance for design.

Currently available probabilistic models for predicting the mechanical failure of MEMS structures are based on classical Weibull statistics. However, existing histogram testings have demonstrated that the strength distributions consistently deviate from those predicted by the two-parameter Weibull distribution. Figure 1 presents, on the Weibull scale, the experimentally measured strength histograms of MEMS structures made of single-crystal Si,[7] hydrogen-free tetrahedral amorphous carbon (ta-C)[6] and poly-Si.[13] It is clear that, even with a limited number of specimens, these histograms cannot be fitted by a straight line on the Weibull scale, indicating that the two-parameter Weibull distribution is inadequate to describe the failure statistics of MEMS devices.[16,17] It should be pointed out that the Weibull distribution can match well the data in the intermediate range of failure probabilities, but fails to capture the tail part of the probability distribution, which is essential for very high reliability structural designs. An attempt to reconcile experimental histogram data with the Weibull approach was proposed using the three-parameter Weibull distribution.[8,14] However, recent studies have pointed out some theoretical deficiencies of the three-parameter Weibull distribution for quasibrittle and brittle materials in terms of its prediction of the scale effect on the mean structural strength.[18,19] Therefore, it has been generally agreed that the existing probabilistic models for brittle MEMS structures are still empirical in nature, which severely limits their predictive capabilities.

This paper presents a robust probabilistic model for MEMS structures that may lead to eliminating the need of less preferable costly proof testing approaches to guarantee the structural safety of devices that will operate at high mechanical power densities and/or large deformation levels. The paper is planned as follows: Section II reviews the classical Weibull statistical model and its key assumptions; Section III presents a generalized weakest link model for MEMS structures; Section IV compares the present model with the existing experimental data on the strength distributions of poly-Si MEMS structures; Section V demonstrates the prediction of failure statistics of MEMS structures under different loading configurations, and Section VI presents the relationship between the mean size effect curve and the strength distribution of MEMS devices, which can be used as an indirect method for determining the failure statistics.

II. Weibull's Weakest Link Model for Material Strength

Weibull's weakest link model is probably the most widely used probabilistic model for brittle material strength.[20–24] We first review this classical model and its underlying assumptions as a motivation for the development of the present model for failure statistics of MEMS structures.

The essence of Weibull's weakest link model is that the structure would fail under a load control condition once one representative material element fails. Such types of structures are often referred to as being of positive geometry. Typical examples include bars under uniaxial tension, beams under flexural loading, and plates under biaxial bending. The overall failure probability of the structure P_f can be related to the failure probability of each representative material element P_1 by the joint probability theorem, that is

$$P_f(\sigma_N) = 1 - \prod_{i=1}^{N}\{1 - P_1[\sigma_N s(\mathbf{x}_i)]\} \tag{1}$$

where $\sigma_N = c_n P_m/bD$ = nominal structural strength, P_m = load capacity of the structure, D = characteristic size of the structure, b = width of the structure in the transverse direction, c_n = constant such that σ_N may carry some physical meaning, e.g. the maximum elastic stress in the structure in the absence of stress concentration, N = number of representative material elements in the structure, $s(\boldsymbol{x}_i)$ = dimensionless stress field such that $\sigma_N s(\boldsymbol{x}_i)$ is equal to the maximum elastic principal stress in the ith material element. Note that Eq. 1 also assumes that the strength of each material element can be treated as a statistically independent random variable.

Weibull considered that the number of representative material elements N is very large. As N becomes large, P_f is determined by the far-left tail of the failure probability distribution of one material element. By rewriting Eq. 1 in a logarithmic form and considering $\ln(1 - x) \approx -x$ $(x \to 0)$, we have

$$\ln[1 - P_f(\sigma_N)] = -\sum_{i=1}^{N} P_1[\sigma_N s(\boldsymbol{x}_i)] \tag{2}$$

Based on experimental observations, Weibull further proposed that the far-left tail of $P_1(x)$ should follow a power law, i.e., $P_1(x) = (x/s_0)^m$. Since N is large, we may replace the sum in Eq. 2 by a volume integral, and Eq. 2 leads to

$$P_f(\sigma_N) = 1 - \exp[-C(\sigma_N/s_0)^m] \tag{3}$$

where $C = l_0^{-n_d}\int_V s^m(\boldsymbol{x})dV(\boldsymbol{x})$, l_0 = size of the representative material element, and n_d = number of spatial dimension of the structure considered in the model. Equation 3 is the well-known two-parameter Weibull distribution, and constants m and s_0 are usually referred to as the Weibull shape parameter (Weibull modulus) and scale parameter, respectively. It should also be mentioned here that from a pure statistics viewpoint the Weibull distribution belongs to the class of extreme value distribution functions, which was first derived mathematically by Fisher and Tippet[25] based on the postulate of stability. Weibull[20] independently proposed this distri-

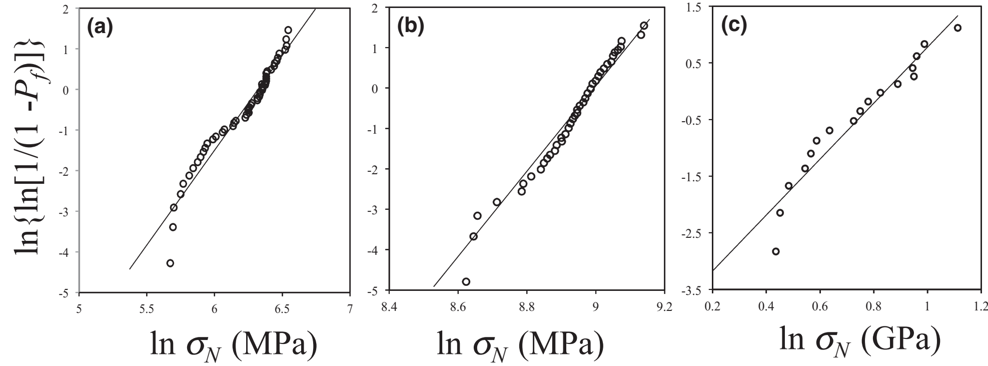

Fig. 1. Experimentally measured strength histograms of MEMS structures made of: (a) single-crystal Si, (b) ta-C, and (c) Poly-Si.

bution function from the weakest link model in conjunction with extensive histogram testing of various engineering materials, such as porcelain, portland cement, wood, and cotton yarn.

Now consider a set of geometrically similar structures of different sizes D. It is clear that these structures would have the same dimensionless elastic stress field expressed by the dimensionless coordinate $\boldsymbol{\xi} = \boldsymbol{x}/D$. Using this dimensionless coordinate, Eq. 3 can be written as

$$P_{\mathrm{f}}(\sigma_N) = 1 - \exp\left[-\Psi \frac{D^{n_{\mathrm{d}}}}{l_0^{n_{\mathrm{d}}}} \left(\frac{\sigma_N}{s_0}\right)^m\right] \quad (4)$$

where $\Psi = \int_V s^m(\xi) \mathrm{d}V(\xi)$. The mean nominal strength can be calculated as

$$\bar{\sigma}_N = \int_0^1 \sigma_N(P_{\mathrm{f}}) \mathrm{d}P_{\mathrm{f}} = \int_0^\infty [1 - P_{\mathrm{f}}(\sigma_N)] \mathrm{d}\sigma_N \quad (5)$$

By substituting Eq. 4 into Eq. 5, we have

$$\bar{\sigma}_N = s_0 \Gamma(1 + 1/m) l_0^{n_{\mathrm{d}}/m} \Psi^{-1/m} D^{-n_{\mathrm{d}}/m} \quad (6)$$

where $\Gamma(x) =$ Eulerian gamma function. As seen from Eq. 6, the mean nominal strength decreases with an increasing structure size as $\bar{\sigma}_N \propto D^{-n_{\mathrm{d}}/m}$. This is the Weibull size effect, which has widely been used to explain the size dependence of material strength. Such a power-law scaling indicates that the problem does not involve any characteristic length, which is evident for Webull's analysis since the size of the representative material element is considered to be negligibly small compared to the structure size, i.e., $N \to \infty$.

In summary, the Weibull distribution is anchored by four fundamental assumptions: (1) the failure of one material representative element triggers the structural failure, i.e., a weakest link model of structural failure; (2) the random strengths of material elements are statistically independent; (3) the failure probability of one material element follows a power law tail; and (4) the structure is much larger than the representative material element. As discussed earlier, the assumption of the weakest link model is generally valid for structures with a positive geometry. The statistical independence of the material strength can be achieved by choosing a material representative element with a size larger than the autocorrelation length of the random strength field. In fact, the stability postulate for any extreme value distribution can be justified for correlated random systems (such as percolation models,[26–28]) using renormalization group methods, which homogenize the system recursively up to a scale (of the material element) where correlations become negligible. The power-law tail of the strength distribution of material element has recently been justified by combining the transition state theory and a multiscale statistical model.[19,29] The last assumption, which is essential for ensuring the Weibull statistics, is often unmentioned in the application of the Weibull distribution to material strength. This assumption implies that the size of the material inhomogeneities must be negligible compared to the overall structure size. This is consistent with the fact that the Weibull distribution can provide an optimum fit of strength histograms of many brittle structures made of fine-grain ceramics. However, in many cases the number of representative material elements in the structure is not sufficiently large to justify the Weibull distribution.

As mentioned earlier, the failure of poly-Si MEMS structures usually initiates from the surface defects (i.e., sidewall grooves), which act as stress concentrators.[8] Therefore, we may consider each of these sidewall grooves as one element in the weakest link model. In typical MEMS structures that are used in laboratory tests, the number of such sidewall grooves is usually on the order of hundreds. This is at least an order of magnitude less than the required number for the Weibull model to be valid. This explains the observed deviation of the measured strength histograms of MEMS structures from the two-parameter Weibull distribution. Furthermore, the Weibull model also does not explicitly account for the randomness of the sidewall grooves, which gives arise to the random local stress field along the sidewall. In view of this, a more general probabilistic model is needed to describe the failure statistics of MEMS structures.

III. Generalized Weakest Link Failure Model

Consider a poly-Si MEMS specimen subjected to uniaxial tension, where the sidewalls of the specimen contain surface grooves resulted from the manufacturing process [Fig. 2(a)]. It is generally accepted that these surface grooves can be approximated by V-notches.[8,30] The applied tensile stress reaches its maximum value σ_N once a localized crack starts to propagate from one of these grooves. Therefore, the overall failure probability of the specimen can be calculated by using the weakest link model, as described by Eq. 1. Here the function $P_1(x)$ in Eq. 1 represents the probability of the propagation of a localized crack from one surface groove. To model the failure statistics of specimens containing a finite number of surface grooves along the sidewall, we would need to know the entire function $P_1(x)$. By contrast, the classical Weibull model only requires knowledge of the far-left tail of $P_1(x)$. Therefore, the present model can be regarded as a generalization of the Weibull model, and herein we refer to it as the finite weakest link model.

It is clear that some kind of failure criterion is needed for computing $P_1(x)$. In this study, we consider that a localized crack would start to initiate and propagate from one surface groove (idealized as a V-notch) once the average tensile stress $\bar{\sigma}$ of the near-tip region reaches the tensile strength f_{t} of the material, where the average tensile stress is defined as

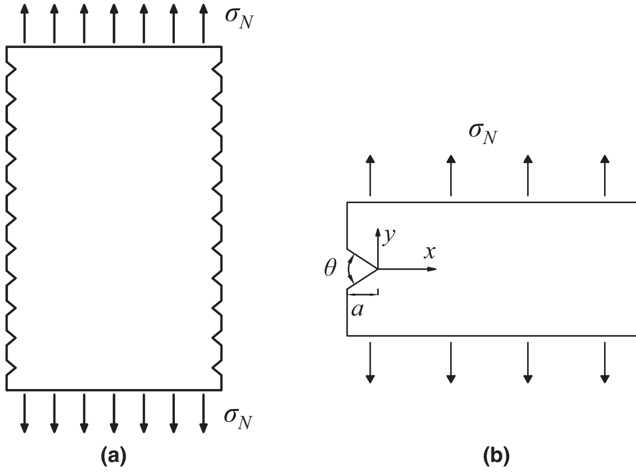

Fig. 2. Analysis of poly-Si tensile specimens: (a) specimen geometry, and (b) criterion of crack initiation from a surface groove.

$$\bar{\sigma} = r_c^{-1} \int_0^{r_c} \sigma_{yy}(x) \mathrm{d}x \tag{7}$$

where $\sigma_{yy}(x)$ = elastic tensile stress along the notch ligament [Fig. 2(b)] and r_c = size of the near-tip region in which the average stress is computed. The present averaging procedure can be considered as a simplified version of the nonlocal approach that accounts for the interaction of the sub-scale damages inside the fracture process zone (FPZ) formed at the V-notch tip prior to crack propagation. Therefore, it is clear that the material tensile strength f_t used in the present failure criterion should be understood as the tensile strength of the material element, whose size is approximately equal to the FPZ size.

In this study, we consider r_c = 5 nm, which is on the order of the estimated FPZ size of silicon.[8,31] The exact value of r_c can be determined by employing detailed atomistic calculations for the near-tip region, which would provide insights into the failure behavior of silicon crystals. As will be discussed later, the choice of r_c will affect the calibration of the probability distribution of the material tensile strength, but not the qualitative behavior of the present model.

Based on the aforementioned failure criterion, the overall tensile strength of the specimen can be calculated as $\sigma_N = f_t/s$, where s = dimensionless stress such that $\sigma_N s = \bar{\sigma}$. Then the probability of crack propagation from one surface groove can be calculated as

$$P_1 = \mathrm{Prob}(\bar{\sigma} \geq f_t) = \mathrm{Prob}(f_t/s \leq \sigma_N) \tag{8}$$

It is expected that the tensile strength of poly-Si would be subjected to a certain level of randomness. According to recent studies on the strength statistics of quasibrittle materials,[19,29,32,33] the probability distribution of the material tensile strength can be approximated by a Gaussian–Weibull grafted distribution function:

$$F_{f_t}(x) = 1 - \exp[-(x/s_0)^m] \approx (x/s_0)^m \qquad (x \leq \sigma_{gr}) \tag{9}$$

$$F_{f_t}(x) = P_{gr} + \frac{r_f}{\sqrt{2\pi}\delta_G} \int_{\sigma_{gr}}^{x} e^{-(x'-\mu_G)^2/2\delta_G^2} \mathrm{d}x' \quad (x > \sigma_{gr}) \tag{10}$$

where m = Weibull modulus (shape parameter), s_0 = Weibull scale parameter, μ_G, δ_G = mean and standard deviation of the Gaussian core, respectively, $P_{gr} = 1 - \exp[-(\sigma_{gr}/s_0)^m]$ = grafting probability at which the Weibull tail ends, and r_f = normalizing parameter, which ensures that $F_{f_t}(\infty) = 1$. Furthermore, the probability density function (pdf) at the Weibull–Gaussian grafting point must be continuous, i.e., $\mathrm{d}P_{f_t}(x)/\mathrm{d}x|_{x=\sigma_{gr}^-} = \mathrm{d}P_{f_t}(x)/\mathrm{d}x|_{x=\sigma_{gr}^+}$.

The Gaussian–Weibull functional form of material strength distribution may be qualitatively explained as follows. When the size of the material element approaches the FPZ size, the material element would exhibit a quasi-plastic failure behavior, and the consequently the strength of the element could be calculated as the sum of strengths of the sub-scale material elements along the failure surface. By virtue of the Central Limit Theorem, the strength of the material element must approach a Gaussian cdf. Meanwhile, it is obvious that the far-left tail of the Gaussian distribution would extend to negative strength values and therefore must be rejected. Recent studies have shown that the probability distribution of material strengths at all material scales should follow a power-law. This power-law tail ensues from the application of the transition state theory to the nanocrack propagation through atomic lattices, where the jump of a nanocrack over one atomic bond can be regarded as the transition between two metastable states.[19,29]

Besides the randomness of material tensile strength, the dimensionless stress s is also a random variable since the geometry of the surface V-notch is subjected to a certain level of uncertainty. Here we assume that the V-notches along the sidewall are noninteracting for calculating the elastic stress field of the near-tip region. Based on this assumption, we may calculate the elastic field for a strip of the specimen that contains a V-notch on one of its sidewalls, as shown in Fig. 2(b). It is noted that the V-notch on the other side has no effect on the near-tip stress field of the V-notch on this side since the width of a typical MEMS specimen (on the order of microns) is much larger than the size of the near-tip region. Therefore, we only need to consider one V-notch to compute the near-tip elastic stress field. Based on the known randomness of surface groove geometry, the geometrical parameters of the V-notch, i.e., the notch angle θ and notch depth a, can be randomized to perform a stochastic analysis of the near-tip stress field, from which we can obtain the probability distribution of the dimensionless stress, $F_s(x)$. It is noted that in this study we did not consider the random crystal orientation since it has recently been shown that the mismatch of silicons (relatively low anisotropy) crystal orientation does not significantly affect the near-tip stress field.[8]

Based on Eq. 8, the probability of crack propagation from one V-notch tip can be directly described by the probability distribution of a random variable $\eta = f_t/s$, i.e., $P_1(\sigma_N) = P_\eta(\sigma_N)$. Since both f_t and s are random variables, Eq. 8 can be re-written as

$$P_1(\sigma_N) = \int_0^\infty F_{f_t}(x\sigma_N) f_s(x) \mathrm{d}x \tag{11}$$

where $f_s(x) = \mathrm{d}F_s(x)/\mathrm{d}x$ = pdf of dimensionless stress s. Therefore, the probability distribution of the tensile strength of the entire specimen can be computed as

$$P_f(\sigma_N) = 1 - \left[1 - \int_0^\infty F_{f_t}(x\sigma_N) f_s(x) \mathrm{d}x\right]^{2n} \tag{12}$$

where n = number of V-notches along one sidewall. It should be emphasized that, when writing Eq. 12, we have assumed that the strength of each material element is statistically independent. Such an assumption is reasonable because the size of the V-notch is considerably larger than the FPZ size, which is approximately on the same order of the

autocorrelation length of random strength field for brittle and quasibrittle materials.[33,34]

We can now easily derive the asymptotic form of $P_f(\sigma_N)$ when the sidewall consists of a large number of V-notches, i.e., $n \to \infty$. In this case, we just need the left-tail part of $P_1(\sigma_N)$ to compute $P_f(\sigma_N)$. Based on Eqs. 9 and 11, the left-tail part of $P_1(\sigma_N)$ can be rewritten as

$$P_1(\sigma_N) = M_m \left(\frac{\sigma_N}{s_0}\right)^m \tag{13}$$

where $M_m = \int_0^\infty x^m f_s(x)\mathrm{d}x = m$th moment of probability distribution function $F_s(x)$. Following the aforementioned Weibull analysis, we can readily conclude that, at the large-size limit, $P_f(\sigma_N)$ must converge to the classical Weibull distribution:

$$P_f(\sigma_N) = 1 - \exp[-2nM_m(\sigma_N/s_0)^m] \tag{14}$$

It is clear that, for the case where the number of V-notches along the sidewall is finite, the strength distribution of the specimen necessarily deviates from the two-parameter Weibull distribution. It is expected that such a transition from non-Weibullian to Weibull strength distribution as a function of the structure size would give arise to an intricate size effect on the mean structural strength, which must be different from the classical Weibull size effect. We will discuss this mean size effect and its implication on reliability analysis in detail in Section VI.

IV. Model Comparisons with Experimental Data

With the recent development of high-throughput testing techniques, more complete information on the strength statistics of MEMS devices including its scale effect is available. Figure 3 shows the measured strength histograms of poly-Si tensile specimens of two gauge lengths (L_g = 20 and 70 μm).[8] These specimens have a nominal width of 2 μm. The specimens of 70 μm gauge length were tested using an on-chip tester,[35] in which the tensile specimen was loaded by an on-chip chevron thermal actuator through a prehensile grip mechanism. The specimens of 20 μm gauge length were tested using a slack-chain tester,[36] in which a series of specimens was placed in a chain and loaded by a custom-built probe station. The detailed experimental procedure for these histogram tests can be found in Ref. [28,35]. It should be pointed out that the present data with a size ratio of 1: 3.5 may not be sufficient to fully justify the predictability of a probabilistic model. Nevertheless, as will be shown later in this section, histograms of such a limited size range have already demonstrated the limitations of the classical Weibull models, and the main features of these existing histograms can be well captured by the present model.

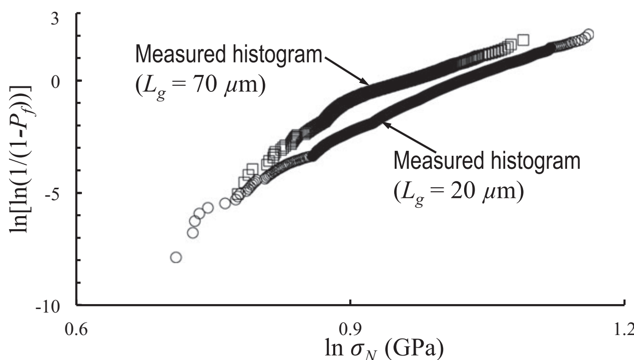

Fig. 3. Measured strength histograms of poly-Si MEMS specimens of two gauge lengths under uniaxial tension.

(1) Finite Weakest Link Model

We now test the present probabilistic model against this set of experimental data. According to Ref. [8] there are approximately 50 surface grooves along one sidewall of the tensile specimen with a gauge length of 20 μm. Therefore, we may consider a strip of specimen with a length of 400 nm subjected to a unit stress ($\sigma_N = 1$) for calculating the random dimensionless stress, s, for the notch-tip region [Fig. 2(b)]. As mentioned earlier, the randomness of the near-tip stress field is expected to be caused by the randomness of the notch angle and depth. In this study, we assume that the notch angle θ follows a uniform distribution bounded between 20° and 140° whereas the notch depth a follows the Type III extreme value distribution for the maximum value with an upper bound of 62 nm.[8] The cdfs of θ and a can be written as

$$F_\theta(x) = \frac{x - 20}{120} \tag{15}$$

$$F_a(x) = \exp\left[-\left(\frac{\langle 62 - x\rangle}{28}\right)^{6.5}\right] \tag{16}$$

where $\langle x\rangle = \max(x,0)$. Note that the assumed probability distribution function of the notch depth extends to negative values, which is physically impossible. However, the left tail for the negative notch depth is extremely short (i.e., $F_a(0) = 6.7 \times 10^{-77}$), which can essentially be neglected in the sampling process. It is also noted that the aforementioned bounds of notch angle and depth ensure that, for any combination of notch angle and depth sampled from the above distributions, the V-notch can always be contained in a 400 nm long strip of the specimen.

Based on the assumed probability distribution functions of the notch angle and depth, we perform stochastic elastic analysis of the stress field for the strip of the tensile specimen, where the random notch angle and depth are sampled by using the Latin Hypercube Sampling technique. The poly-Si material is modeled as an isotropic material with a Young Modulus E = 156 GPa and a Poisson ratio ν = 0.22.[8] Figure 4(a) presents the simulated tensile stress profile along the notch ligament for the realization with θ = 120° and a = 40 nm. Through a sufficient number of realizations, we obtain the pdf of the dimensionless stress, $f_s(x)$, as shown in Fig. 4(b), based on the calculated stress profile.

The probability distribution function of material strength, $F_{f_t}(x)$, needs to calibrated by optimum fits of the measured strength histograms. Since we have strength histograms of specimens of two gauge lengths, we choose one of them to calibrate the function $F_{f_t}(x)$ (Fig. 5) and compare the other one with the model prediction. Table I presents the statistical parameters of $F_{f_t}(x)$ calibrated by optimum fits of (1) strength histogram of specimens of 20 μm gauge length, and (2) strength histogram of specimens of 70 μm gauge length. It can be seen that these two calibrations yield very similar values of the parameters of $F_{f_t}(x)$, which indicates the consistency of the proposed model.

Figure 6 compares the measured strength histogram of the specimens that is not used for model calibration with the prediction by the present model. It is seen that, regardless of which specimen length is used for calibration, the present model can predict reasonably well the strength distribution of specimens of the other gauge length. This indicates that the present model is able to capture the size effect on the strength distribution of poly-Si MEMS specimens, which is essential for reliability-based design extrapolation across different specimen sizes. Furthermore, it is interesting to note that the calibrated mean strength of each material element is about 20 GPa, which is of the order of the theoretical strength of silicon.[37] It should also be pointed out that the

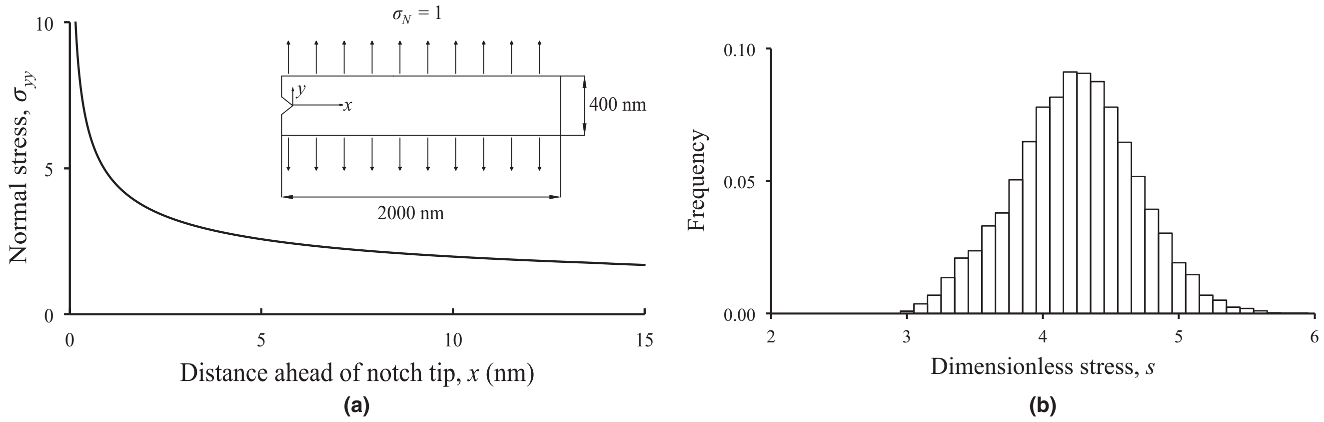

Fig. 4. Stress analysis of near-tip region of the V-notch: (a) a typical stress profile along the ligament of the notch; and (b) simulated probability distribution of dimensionless stress s.

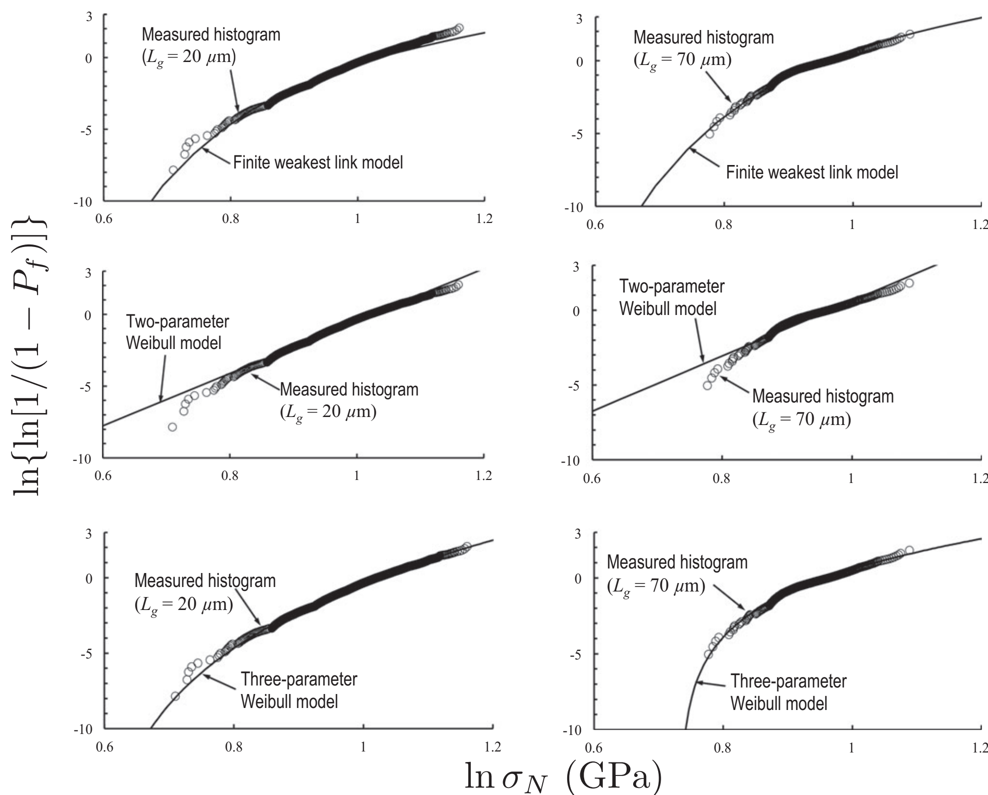

Fig. 5. Optimum fits of the measured strength histograms of poly-Si tensile specimens by the finite weakest link model and the two-parameter and the three-parameter Weibull distributions.

Table I. Calibrated Statistical Parameters of the Finite Weakest Link Model

Tensile specimens used for calibration	m	s_0 (GPa)	μ_G (GPa)	δ_G (GPa)	P_{gr}	r_f
Specimens with $L_g = 20\mu m$	64	12.60	19.96	3.50	9.40×10^{-4}	1.0057
Specimens with $L_g = 70\,\mu m$	65	12.79	19.84	3.40	1.02×10^{-3}	1.0061

calibration of function $F_{f_t}(x)$ depends on the size of the near-tip region r_c. As mentioned earlier, we choose $r_c = 5$ nm based on the knowledge of the FPZ size, and it gives a reasonable estimation of the mean strength of the material element of poly-Si. If another value of r_c was chosen, which would effectively change the value of the dimensionless stress field, the functional form of the overall failure probability $P_f(\sigma_N)$ would not be affected and therefore we expected that Eq. 12 can still match the histograms well. However, the corresponding values of the parameters for function $F_{f_t}(x)$ would be different.

From Table I, it is seen that the fitted value of Weibull modulus is very high. It is noted that the recently developed probabilistic model, which yields the Weibull–Gaussian functional form of the strength distribution of one material element, predicts that the Weibull modulus of material strength distribution at the nanoscale should be equal to two, and it would gradually increase as we move up to the

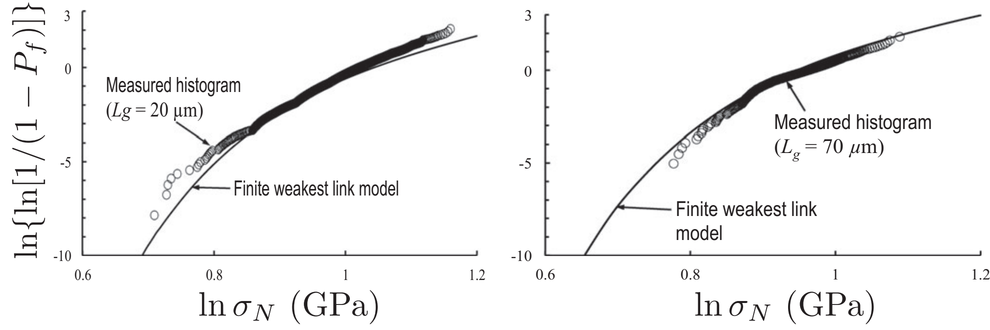

Fig. 6. Comparison between the experimental measured strength histogram of poly-Si MEMS specimens with the prediction by the finite weakest link model.

macoscale,[19,29], for example, the Weibull modulus of concrete at the macroscale is 24. Therefore, it is an intriguing question why the microscale poly-Si MEMS devices would exhibit such a high Weibull modulus, which deserves further in-depth studies. One promising means for such investigations is to use a realistic atomistic simulation tool, such as stochastic quasi-continuum model, which will provide insights into various nonlinear mechanisms as well as random microstructural properties that could possibly lead to a high Weibull modulus.

(2) Two-Parameter Weibull Distribution

As a comparison, we also test the commonly used two-parameter Weibull distribution against this data set. Based on Eq. 3, the two-parameter Weibull distribution for tensile specimens can be written as

$$P_{w2}(\sigma_N) = 1 - \exp[-2n(\sigma_N/s_w)^{m_w}] \tag{17}$$

where s_w = Weibull scaling parameter and m_w = Weibull modulus. The values of s_w and m_w can be easily obtained by plotting the measured strength histogram on the Weibull scale and fitting it by a straight line. Similar to the aforementioned calibration procedure, we determine s_w and m_w by optimum fitting either one of the two strength histograms and compare the other histogram with that predicted by Eq. 17. Table II lists the values of s_w and m_w determined by fitting the strength histograms of specimens of either of the two gauge lengths. It can be seen that the calibrated values do not strongly depend on which strength histogram is used for fitting. However, similar to Fig. 1, we can see from Fig. 5 that these histograms cannot be optimally fitted by a straight line on the Weibull scale. Fig. 7 presents the predicted strength histogram of specimens of the other gauge length by the two-parameter Weibull distribution with the experimental data. Clearly, for either of the two calibrations, the two-parameter Weibull distribution cannot well predict the strength distribution of specimens. The deviation from the experimental measurement indicate that the two-parameter Weibull distribution is insufficient for modeling the failure statistics of general poly-Si MEMS specimens. As discussed, the physical reason for such a deviation is that for these two sets of test specimens the number of potential failure points (i.e., V-notches) inside the specimen is not sufficiently large to grant the validity of the Weibull distribution.

(3) Three-Parameter Weibull Distribution

The three-parameter Weibull distribution has recently been proposed as a remedy for the two-parameter Weibull distribution, in which it introduces a finite strength threshold under which the structure will never fail. The three-parameter Weibull distribution for tensile specimens can be written as

$$P_{w3}(\sigma_N) = 1 - \exp\left[-2n\frac{\langle\sigma_N - \sigma_0\rangle^{m_1}}{{s_1}^{m_1}}\right] \tag{18}$$

where σ_0 = strength threshold. We can determine m_1, s_1 and σ_0 by fitting the strength histogram of specimens of any size. Table II presents the two sets of values of these three parameters by optimum fitting of the strength histograms of specimens of 20 and 70 μm gauge lengths, respectively. The optimum fitting is shown in Fig. 5. It can be seen that the calibration result is strongly dependent on the choice of the strength histogram for fitting.

Figure 8 compares the predicted strength histogram of specimens that is not used for fitting with the experimental result. It is interesting to see that, if we calibrate m_1, s_1 and σ_0 based on the strength histogram of specimens of 20 μm gauge length, Eq. 18 can predict well the strength distribution of specimens of 70 μm gauge length. On the contrary, if we calibrate m_1, s_1 and σ_0 based on the strength histogram of specimens of 70 μm gauge length, Eq. 18 fails to predict the strength distribution of specimens of 20 μm gauge length. This illustrates the lack of robustness of the

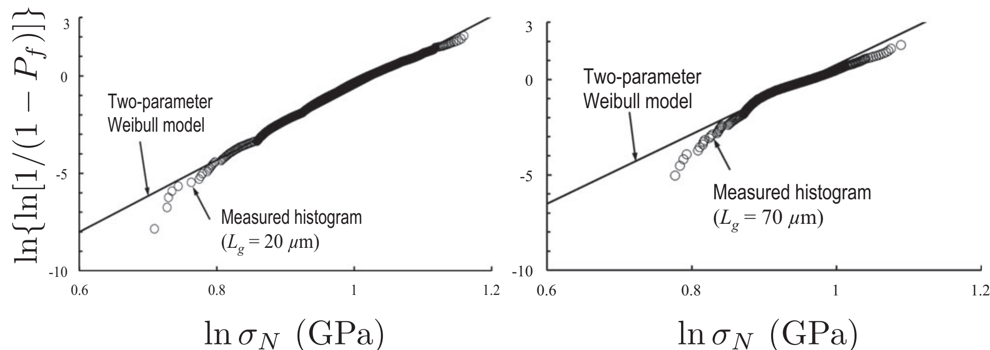

Fig. 7. Comparison between the experimental measured strength histogram of poly-Si MEMS specimens with the prediction by the two-parameter Weibull distribution.

Table II. Calibrated Statistical Parameters of the Two-Parameter and Three-Parameter Weibull Distributions

Tensile specimens used for calibration	m_w	s_w (GPa)	m_1	s_1(GPa)	σ_0 (GPa)
Specimens with $L_g = 20\,\mu m$	18.25	3.59	5.78	2.22	1.78
Specimens with $L_g = 70\,\mu m$	18.45	3.61	3.03	3.66	2.08

three-parameter Weibull distribution for prediction of failure statistics of specimens of different sizes, since its prediction capacity is dependent on which histogram is used for calibration.

Meanwhile, it should be pointed out that the three-parameter Weibull distribution has recently been shown theoretically unsound for strength statistics of brittle and quasibrittle structures because (1) it predicts an incorrect size effect on the mean structural strength at the large size limit,[18,38] and (2) the strength threshold is theoretically unjustifiable since the probability distribution of the material strength should have a power-law with zero threshold as implied by the transition state theory.[19]

It may be concluded that the aforementioned comparison with the experiment data on poly-Si tensile specimens of two different gauge lengths favors the present finite weakest link model over the classical two- and three-parameter Weibull distributions, even though the size range of the experimental data is narrow. It is interesting to compare the strength distributions of tensile specimens for a wider range of gauge lengths predicted by the present finite weakest link model and the three-parameter Weibull distribution, as shown in Fig. 9. It can be seen that for $n = 50$ two models give a reasonably similar prediction of the failure probability except for the tail part since these two models are calibrated based on the test results for specimens of 20 μm gauge length. At the small-size limit, it is observed that these two models only differ at the high-probability regime and the extreme far left tail. At the large-size limit, these two models give a similar prediction for the high-probability regime and they deviate from each other significantly at the low probability regime.

The aforementioned observation can be explained by the fact that the strength distribution for the high probability regime of large-size structures is determined by the strength distribution for the low probability regime of small-size structures, which is an essential feature of the weakest link model. This is why we just need the far left tail of the strength distribution of material element to derive the classical Weibull distribution. As seen in Fig. 9(b), the finite weakest link model and the three-parameter Weibull distribution give a similar prediction for the bulk part of the strength distribution for $n = 50$, we can expect that these models would also lead to a similar prediction of the strength statistics at the low probability regime for $n = 1$, as seen Fig. 9(a). Meanwhile, we do see that these two models differ from each other at the extremely low failure probability regime as well as the high probability regime. As n increases from 50, we see that the difference in prediction by these models starts to propagate into the intermediate and high probability regime. This is simply because that the difference in the tail behaviors predicted by these two models is manifested in the different behavior of the bulk part of the strength distribution as the specimen size increases.

In Fig. 9, we present the design strengths corresponding to two tolerable risk levels, i.e., $P_f = 10^{-4}$ or 10^{-6}. It can be seen that these two models give a similar prediction of the design strengths for these two risk levels except for the large size limit, where the three-parameter Weibull model would underestimate the design strength. This may be the reason why the three-parameter Weibull distribution is an attractive choice since most applications of MEMS structures lie in the intermediate size range. However, as will be discussed in the next section, these models will give very different prediction if we extrapolate to different loading configurations. Meanwhile, it should emphasized here that, even if we are interested in the design strength of tensile specimens of small and intermediate sizes, the application of the three-parameter Weibull distribution is still hampered by the aforementioned ambiguity of the calibration results.

It is also worthwhile to point out that, in contrast to the three-parameter Weibull distribution, which leads to an overestimation of the design strength, the optimally fitted two-parameter Weibull distribution would underestimate the design strength at $P_f = 10^{-4}$ or 10^{-6}. The predicted design strength could be 30% lower than that predicted by the finite weakest link model, which would lead to an expensive design. Furthermore, we will demonstrate in the next section that the two-parameter Weibull distribution may not yield a conservative design where we extrapolate the results to different loading configurations.

V. Design Extrapolations for Specimens Under Different Loading Configurations

The previous section focused on the extrapolation of strength statistics of tensile specimens across different specimen sizes. In the actual applications, MEMS devices may be subjected to different loading configurations. It is practically impossible to develop test apparatus for wide ranging loading configurations. Therefore, we have to rely on probabilistic models to facilitate design extrapolation for specimens under different loading. As a demonstration, we apply the present model to predict the failure statistics of poly-Si beams under three-point bending based on the parameters calibrated by the aforementioned tensile experiments.

Consider a poly-Si beam under three-point bending (Fig. 10). We define the nominal strength of the beam as $\sigma_N = 3P_mL/2bD^2$, where P_m = load capacity of the beam,

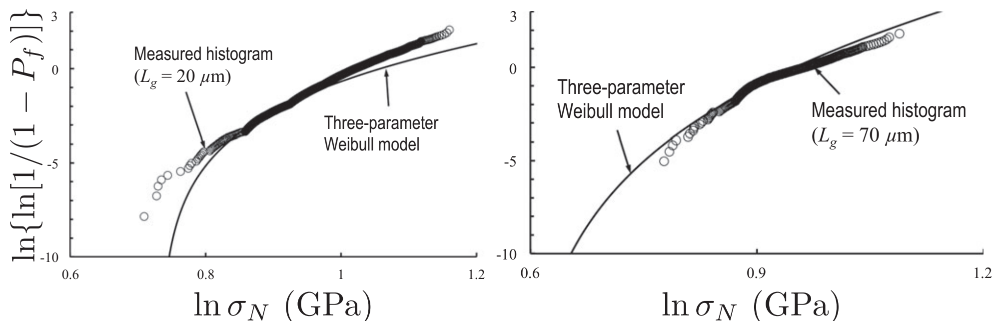

Fig. 8. Comparison between the experimental measured strength histogram of poly-Si MEMS specimens with the prediction by the three-parameter Weibull distribution.

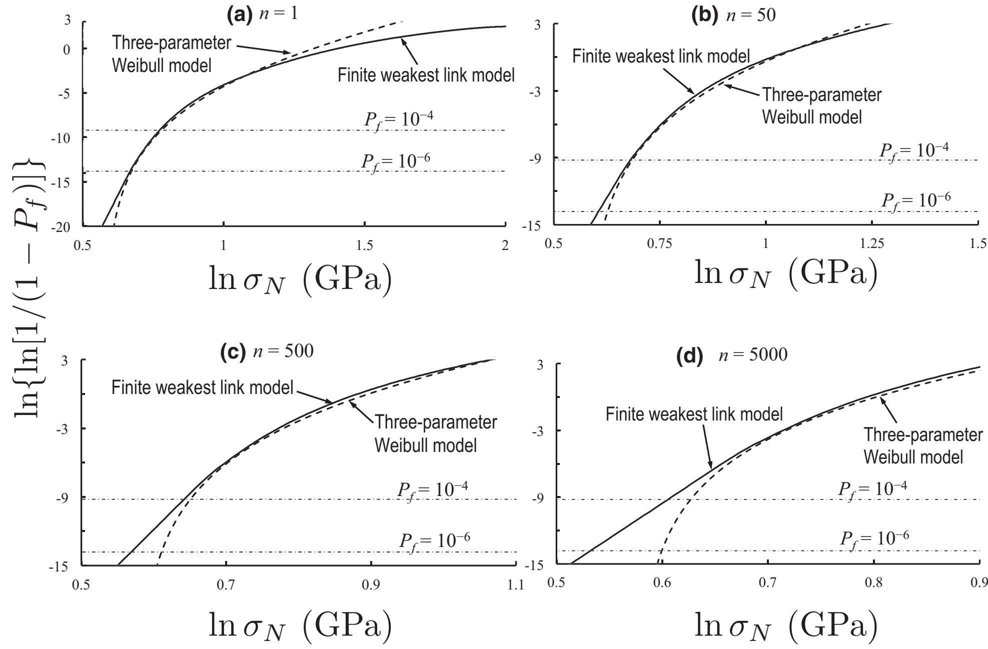

Fig. 9. Comparison of the predicted strength distributions of poly-Si MEMS specimens of different gauge lengths by the finite weakest link model and the three-parameter Weibull distribution: (a) $n = 1$, (b) $n = 50$, (c) $n = 500$, and (d) $n = 5000$.

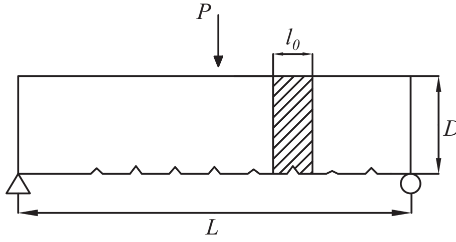

Fig. 10. Geometry of a poly-Si MEMS specimens under flexural loading.

$L =$ beam length, $D =$ beam depth, and $b =$ width of the beam in the transverse direction. For the present calculations, we consider a set of geometrically similar beams with $L/D = 4$ and different lengths $L = 4.8, 10, 20, 40, 80$ μm. It can be well expected that the failure would initiate from the bottom surface of the beam due to the higher bending stress as well as the stress concentrations at the surface grooves (Fig. 10). Meanwhile, due to the random material tensile strength and the geometry of the surface grooves, the failure initiation location is uncertain.

Similar to the tensile specimens, beams under three-point bending also belong to the class of structures of positive geometry. Therefore, we may consider that the beam reaches its load capacity as long as a localized crack initiates from one of the surface grooves along the bottom surface of the beam. Therefore, the overall failure statistics of the beam can be calculated using the weakest link model, where the beam can be considered to consist of a number of vertical material strips, each of which contains a V-notch (Fig. 10). As mentioned in the previous section, the width of these material strip, denoted by l_0, is equal to 400 nm. Different from the foregoing analysis of tensile specimens, these material strips are subjected to nonuniform bending moments and shear forces. In this study, we perform finite element (FE) simulations of the entire beam to compute the near-tip stress fields for all V-notches along the bottom surface. By separating the random geometrical parameters from the random material strength, we may calculate the strength distribution of the entire beam as

$$P_{\mathrm{f}}(\sigma_N) = \int_{\tilde{a},\tilde{\theta}} P_{\mathrm{f}}(\sigma_N)|_{\tilde{a},\tilde{\theta}} f(\tilde{a},\tilde{\theta})\mathrm{d}\tilde{a}\mathrm{d}\tilde{\theta} \tag{19}$$

$$= \mathrm{E}\left[P_{\mathrm{f}}(\sigma_N)|_{\tilde{a},\tilde{\theta}}\right] \tag{20}$$

where $\tilde{a}, \tilde{\theta} =$ random vectors containing the values of depth and angle for all V-notches along the bottom surface, respectively, $f(\tilde{a},\tilde{\theta}) =$ joint pdf of the random notch depth and angle, $P_{\mathrm{f}}(\sigma_N)|_{\tilde{a},\tilde{\theta}} =$ conditional failure probability of the beam for a given set of values of $\tilde{a}$ and $\tilde{\theta}$, and $\mathrm{E}(x) =$ expectation of x. It is clear that the conditional failure probability can be calculated using the weakest link model, i.e.,

$$P_{\mathrm{f}}(\sigma_N)|_{\tilde{a},\tilde{\theta}} = 1 - \prod_{i=1}^{n}\left[1 - F_{f_t}\left(\sigma_N s_i|_{\tilde{a},\tilde{\theta}}\right)\right] \tag{21}$$

where $n = L/l_0$, $s_i|_{\tilde{a},\tilde{\theta}} =$ dimensionless stress for ith V-notch such that $\sigma_N s_i$ is equal to the average tensile stress $\bar{\sigma}$ of near-tip region of this notch, as defined by Eq. 7. In this study, we numerically estimate the expectation of $P_{\mathrm{f}}(\sigma_N)|_{\tilde{a},\tilde{\theta}}$ as

$$\mathrm{E}\left[P_{\mathrm{f}}(\sigma_N)|_{\tilde{a},\tilde{\theta}}\right] = \frac{1}{N_{\mathrm{r}}}\sum_{i=1}^{N_{\mathrm{r}}} P_{\mathrm{f}}(\sigma_N)|_{\tilde{a}_i,\tilde{\theta}_i} \tag{22}$$

where $N_{\mathrm{r}} =$ number of realizations. For each realization, we determine the dimensionless stress field through elastic FE simulations, where the notch angle and depth are sampled from their probability distributions as described by Eqs. 15 and 16. We terminate the calculation once the computed expectation value converges to a relative error less than 5%.

As a comparison, we also calculate the strength distribution of the poly-Si beams by using the two- and three-parameter Weibull distributions. The two-parameter Weibull distribution for structures with a nonuniform stress field is given by Eq. 3. Since we only consider possible failure along the bottom surface, which has a linear stress profile for the half-span, Eq. 3 can be re-written as

$$P_{\mathrm{f}}(\sigma_N) = 1 - \exp\left\{-2l_0^{-1}\left[\int_0^{L/2}(2x/L)^{m_{\mathrm{w}}}\mathrm{d}x\right]\frac{\sigma_N^{m_{\mathrm{w}}}}{s_{\mathrm{w}}^{m_{\mathrm{w}}}}\right\} \quad (23)$$

$$= 1 - \exp\left[-\frac{L}{l_0(m_{\mathrm{w}}+1)}\left(\frac{\sigma_N}{s_{\mathrm{w}}}\right)^{m_{\mathrm{w}}}\right] \quad (24)$$

For the three-parameter Weibull distribution, a similar expression can be derived except that a strength threshold σ_0 is introduced. The probability distribution of the nominal strength of the beam can be expressed as

$$P_{\mathrm{f}}(\sigma_N) = 1 - \exp\left[-s_1^{-m_1}\int_V \langle \sigma_N s(\boldsymbol{x}) - \sigma_0\rangle^{m_1}\mathrm{d}V(\boldsymbol{x})\right] \quad (25)$$

$$= 1 - \exp\left[-\frac{L}{l_0(m_1+1)}\left\langle 1 - \frac{\sigma_0}{\sigma_N}\right\rangle^{m_1+1}\left(\frac{\sigma_N}{s_1}\right)^{m_1}\right] \quad (26)$$

Figure 11 presents the comparison of the strength histograms of this set of geometrically similar poly-Si beams predicted by the finite weakest link model, and the two- and three-parameter Weibull distributions, where all the model parameters are based on the calibration results obtained by optimum fitting of the tensile specimens of 20 μm gauge length. It is seen that the predictions by these models differ from each other for beams of all sizes. The difference is much more significant compared to that for tensile specimens, even though the bending specimens have a similar characteristic size as the tensile specimens. This can be explained by the fact that the nonuniform stress field effectively changes the structure size for the calculation of the failure probability. For example, let us consider the two-parameter Weibull distribution. Comparing Eq. 24 with Eq. 17, it is clear that for calculating the failure probability the specimen under three-point bending is equivalent to the tensile specimen with a gauge length being m_{w} times smaller than the beam length. In other words, we may view that the three-point bend specimens are equivalent to tensile specimens of a much smaller size. Now consider the present finite weakest link model. Unlike the two-parameter Weibull distribution, here the equivalent size of the tensile specimen cannot be calculated analytically. However, based on Eq. 13, it is clear that tail of the strength distribution must follow a Weibull distribution. Therefore, we can still use the aforementioned equivalent size implied by the Weibull distribution for calculating the tail distribution of the nominal strength of the beam. As seen from Tables I and II, the Weibull modulus for the present model and the two-parameter Weibull distribution differ significantly from each other (i.e., $m \gg m_1$) . This implies that for the same bending specimen the equivalent tensile specimen size implied by the two-parameter Weibull distribution is much larger than that implied by the present model, which leads to a large difference in the predicted strength distributions, as shown in Fig. 11.

The foregoing analysis indicates that, even though for tensile specimens the finite weakest link model and three-parameter Weibull distributions may predict a similar design strength corresponding to a failure probability that is not too low (Fig. 9), it does not mean that these distributions are equally good for the same specimens subjected to other loading configurations. This is because the change of the stress field can lead to a drastic change in the equivalent specimen size, and these distributions can give very different predictions of this equivalent specimen size. Therefore, empirical fitting of histogram of specimens of one size or under one loading configuration is usually insufficient for design extrapolation across different specimen sizes and loading configurations.

For the viewpoint of design of MEMS devices, Fig. 11 indicates that the conventional Weibull models would provide a conservative design since they predict a higher failure probability for a given applied load. However, it should be emphasized here that the present analysis considers the prediction of the strength distribution of three-point bending specimens from the measured strength distribution of tension specimens. If we want to extrapolate from three-point bending specimens to tension specimens, it is clear that the conventional Weibull models would overestimate the design strength for a given failure probability compared to the finite weakest link model. Therefore, it should be cautioned that, for design extrapolation across different specimen geometries and loading configurations, the conventional Weibull models does not always yield a conservative design.

It is also clear from our analysis that, to directly validate a probabilistic model for structural strength, we need to per-

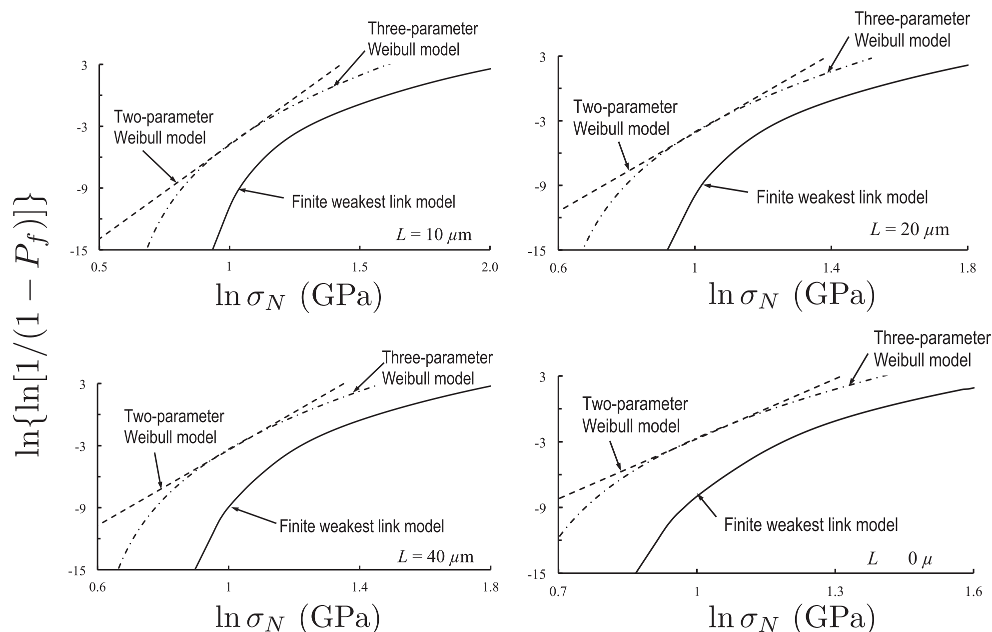

Fig. 11. Strength distributions of poly-Si bending specimens predicted by the finite weakest link model, and the two- and three-parameter Weibull distributions.

form histogram testing of geometrically similar specimens with a sufficiently large size range. This approach has two main advantages: (1) it can provide a more complete model validation against the size dependence of the strength distribution, which is essential for design extrapolation across different specimen sizes and geometries; and (2) it can eliminate the need to experimentally measure the far-left tail of the strength distribution because the tail behavior would be reflected within the bulk part of the strength distribution of large-size specimens. Of course the main challenge of the size effect tests is that it is sometimes difficult to achieve a large size range because the size of the test specimens is limited by the test set-up. In such a case, according to the aforementioned analysis, we may change the loading configurations to create different stress fields so that we can effectively achieve a large size range for the same set of specimen sizes. For example, to achieve the large-size limit for bending specimens, we may perform uniaxial tension tests on the specimens of the same size, and on the contrary, to achieve the small-size limit for tensile specimens, we may perform three-point bending tests on the specimens of the same size.

VI. Mean Size Effect Curve and Strength Distribution

Based on the foregoing analysis in Section IV, it is seen that the present finite weakest link model agrees well with the the measured strength histograms of poly-Si tensile specimens of different gauge lengths and the model calibration is subjected to a level of minimal ambiguity. As mentioned earlier, the finite weakest link model (Eq. 12) predicts that the probability distribution of structural strength is strongly dependent on the structure size, and the direct consequence is a size effect on the mean structural strength. In this section, we explore the relationship between this mean size effect and the strength distribution. The direct implication of this relationship is that it would allow us to determine the strength distribution directly from the size effect curve of the mean strength. This concept of determination of strength distribution based on the mean size effect analysis has recently been proposed and tested for quasibrittle structures.[39,40] Such an indirect method would potentially eliminate the need of histogram testing for reliability analysis of MEMS devices. Instead, we would just need to obtain the size effect curve of the mean structural strength, which would involve specimens of four to five sizes (or loading configurations). For each specimen size (or loading configuration), only five specimens would be needed for determining the mean strength. Therefore, the total number of specimens involved in the test is significantly lower than that involved in conventional histogram testing. Here we formulate the relationship between the mean size effect curve and the strength distribution for the aforementioned tension specimens, while the same formulation can directly be applied to structures of other geometries or under other loading configurations.

Based on Eq. 12, the mean structural strength can be calculated as

$$\bar{\sigma}_N = \int_0^1 \sigma_N \mathrm{d}P_\mathrm{f}(\sigma_N) = \int_0^\infty \left[1 - \int_0^\infty F_{f_\mathrm{t}}(x\sigma_N) f_\mathrm{s}(x)\mathrm{d}x\right]^{2n} \mathrm{d}\sigma_N \quad (27)$$

We note that the randomness of V-notch geometry can be accurately determined from the examination of the surface grooves along the sidewalls, and the probability distribution of the dimensionless stress, $f_\mathrm{s}(x)$, can then be calculated from the stochastic elastic FE simulations. Therefore, the crux of the problem is to determine the probability distribution of the material element strength, i.e., $F_{f_\mathrm{t}}(x)$, from the mean size effect curve.

Figure 12 presents the size effect on the tensile specimens calculated by Eq. 27, where $F_{f_\mathrm{t}}(x)$ is calibrated based on the strength histogram of specimen of 20 μm gauge length. It is seen that, on the log–log scale, the mean size effect curve deviates from the Weibull size effect, which would follow a straight line on this plot. Within the present framework, this is clearly due to the fact that there is a finite number of V-notches along the sidewalls. As expected, when the specimen length becomes large, the mean size effect does follow the Weibull size effect. Though Eq. 27 cannot be integrated analytically, we may construct a general approximate equation for $\bar{\sigma}_N$ by anchoring at the small- and large-size limits:[19,41,42]

$$\bar{\sigma}_N = \mu_0 \left[\frac{n_1}{n} + \left(\frac{n_2}{n}\right)^{r/q}\right]^{1/r} \quad (28)$$

where μ_0 = mean strength of material element, and n_1, n_2, r, and q are constants. Let us denote $C_1 = \mu_0^r n_1$ and $C_2 = \mu_0^q n_2$. Now we relate these constants to the probability distribution function of material strength $F_{f_\mathrm{t}}(x)$. Based on Eqs. 9 and 10 , $F_{f_\mathrm{t}}(x)$ can uniquely be defined by the following four parameters: the Weibull modulus m, the Weibull scaling parameter s_0, the mean of the Gaussian core μ_G, and the standard deviation of the Gaussian core δ_G.

At the large size limit, the strength distribution of the structure must converge to the Weibull distribution [Eq. (14)]. The corresponding mean structural strength can be easily obtained:

$$\bar{\sigma}_N = (2n)^{-1/m} s_0 \Gamma(1 + 1/m) M_m^{-1/m} \quad (29)$$

On the other hand, as $n \to \infty$, Eq. 28 reduces to $\bar{\sigma}_N \approx \mu_0 (n_2/n)^{1/q}$. Comparing this expression with Eq. 29, we obtain

$$m = q \quad (30)$$

$$s_0 = (2M_m)^{1/m} C_2^{1/q} \Gamma^{-1}(1 + 1/m) \quad (31)$$

This implies that constants q and C_2 are directly related to the Weibull modulus and the Weibull scaling parameter.

At the small-size limit, the entire specimen consists of only two V-notches, one on each sidewall. It is well expected that the Weibull tail can be neglected for calculating the mean strength. Therefore, we may replace the Weibull–Gaussian grafted strength distribution by a Gaussian distribution to compute the mean strength at the small-size limit, i.e.,:

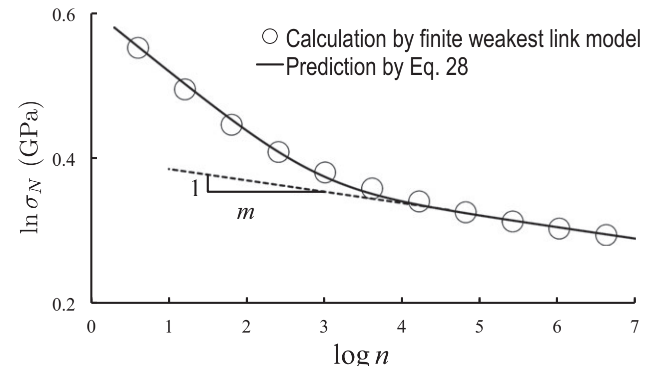

Fig. 12. Comparison of the size effect on the mean structural strength calculated by the finite weakest link model and Eq. 28.

$$\bar{\sigma}_N\big|_{n=1} = \int_0^1 \sigma_N \mathrm{d}P_f = \int_0^\infty \left[1 - \int_0^\infty \Phi\left(\frac{x\sigma_N - \mu_G}{\delta_G}\right) f_s(x)\mathrm{d}x\right]^2 \mathrm{d}\sigma_N \tag{32}$$

where $\Phi(x) =$ standard Gaussian distribution. Meanwhile, we can also calculate the derivative of $\bar{\sigma}_N$ with respect to the number of V-notches at the small-size limit:

$$\frac{\mathrm{d}\bar{\sigma}_N}{\mathrm{d}n}\bigg|_{n=1} = \int_0^\infty \left[1 - \int_0^\infty \Phi\left(\frac{x\sigma_N - \mu_G}{\delta_G}\right) f_s(x)\mathrm{d}x\right]^2 \ln\left[1 - \int_0^\infty \Phi\left(\frac{x\sigma_N - \mu_G}{\delta_G}\right) f_s(x)\mathrm{d}x\right] \mathrm{d}\sigma_N \tag{33}$$

Based on Eq. 28, these two small-size asymptotes can be written as

$$\bar{\sigma}_N\big|_{n=1} = (C_1 + C_2{}^{r/q})^{1/r} \tag{34}$$

$$\frac{\mathrm{d}\bar{\sigma}_N}{\mathrm{d}n}\bigg|_{n=1} = -\frac{1}{r}(C_1 + C_2{}^{r/q})^{1/r-1}\left(C_1 + \frac{rC_2{}^{r/q}}{q}\right) \tag{35}$$

It is clear that, by equating Eqs. 32 to Eq. 34 and Eq. 33 to Eq. 35, we can calculate μ_G and δ_G from C_1, C_2, r and q. Therefore, if we obtain a size effect curve on the mean structural strength and we fit it with Eq. 28, we can use the foregoing formulation to determine s_0, m, μ_G and δ_G, from which we can further calculate the strength distributions of the tensile specimens of different sizes by using Eq. 12 as well as specimens of other geometries or under other loading configurations by using Eq. 19.

We now use the current data on poly-Si tension specimens to verify the aforementioned formulation. Since we have calibrated the strength distribution of material element, i.e., s_0, m, μ_G and δ_G, we can directly calculate constants q, r, μ_0, n_1 and n_2 based on Eqs. 30–35 and obtain an approximate size effect curve using Eq. 28. Figure 12 shows that the approximated size effect predicted by Eq. 28 agrees well with the calculated size effect on the mean strength of tensile specimens, which verifies the proposed relationship between the mean size effect curve and the strength distribution.

VII. Conclusions

1. The measured strength histograms of poly-Si MEMS specimens of two gauge lengths can be well explained by a finite weakest link model, which explicitly accounts for both the random material strength and random geometrical features of the specimen. The model can be calibrated by optimum fitting of either one of these two strength histograms, and the choice of the histogram for fitting has a minimal effect on the calibration results.
2. It is shown that the two-parameter Weibull distributions cannot predict the measured strength histograms of the two sets of poly-Si specimens, due to the fact that the number of potential failure locations in the specimen is not large, thus violating the basic assumption of the Weibull distribution. The three-parameter Weibull distribution can improve the optimum fitting. However, the model calibration is dependent on the choice of the histogram for fitting, which severely limits its prediction capability.
3. Due to the size dependence of strength statistics of MEMS structures, direct experimental validation of the strength distribution using histogram testing must involve specimens of different sizes, where the size range should be sufficiently large. By adopting such a size effect test procedure, it is unnecessary to directly measure the tail of the distribution, which is implied by the bulk part of the strength distribution of large-size specimens. In experiments, the large size range can be achieved by either changing the physical size of the specimen or changing the loading configuration (or equivalently the stress field).
4. The finite weakest link model predicts a strong size effect on the strength distribution as well as the mean structural strength. It is shown that the size effect curve of the mean strength can directly be related to the strength distribution. This provides us an efficient way to determine the strength statistics of MEMS structures without relying on the laborious histogram testing, which will greatly reduce the cost for the reliability analysis of MEMS structures.

Acknowledgments

The authors gratefully acknowledge the financial support from the U.S. National Science Foundation for this research through Grant NSF/CMMI-1361868. The authors also thank Dr. Brad Boyce (Sandia National Laboratories) for fruitful discussions and providing the experimental data.

References

[1]S. Bart, J. Chang, T. Core, and L. Foster, "Design Rules for a Reliable Surface Micromachined IC Sensor," 33rd *Annual Proc. IEEE Reliability Phys.*, 311–7 (1995).

[2]M. R. Douglass, "Lifetime Estimates and Unique Failure Mechanisms of the Digital Micromirror Device (DMD)," 36th *Annual Proc. IEEE Reliability Phys.*, 9–16 (1998).

[3]B. L. Boyce, R. Ballarini and I. Chasiotis, "An Argument for Proof Testing Brittle Microsystems in High-Reliability Applications," *J. Micromech. Microeng.* **18**, 117001, 4pp (2008).

[4]L. Jiang and M. Spearing, "A Reassessment of Materials Issues in Microelectromechanical Systems (MEMS)," *J. Indian Inst. Sci.* **87** [3] 363–85 (2007).

[5]R. Ballarini, Contributive Research & Development Volume 130: The Role of Mechanics in Microelectromechanical Systems (MEMS) Technology, Air Force Research Laboratory Report, Rep. No. AFRL-ML-WP-TR-1998-4209, 1998.

[6]H. D. Espinosa, et al., "A Comparison of Mechanical Properties of Three MEMS Materials - Silicon Carbide, Ultrananocrystalline Diamond, and Hydrogen-Free Tetrahedral Amorphous Carbon (Ta-C)"; Proceedings of the 11th International Conference on Fracture, Turin, Italy, 2005.

[7]A. M. Fitzgerald, D. M. Pierce, B. M. Huigens, and C. D. White, "A General Methodology to Predict the Reliability of Single-Crystal Silicon MEMS Devices," *J. Microelectromech. Systems*, **18** [4] 962–70 (2009).

[8]E. D. ReedyJr., B. L. Boyce, J. W. Foulk, III, R. V. FieldJr., M. P. de Boer, and S. S. Hazra, "Predicting Fracture in Micrometer-Scale Polycrystalline Silicon MEMS Structures," *J. Microelectromech. Syst.* **20** [4] 922–32 (2011).

[9]R. Ballarini, H. Kahn, A. H. Heuer, M. P. de Boer, and M. T. Dugger, "MEMS Structures for On-Chip Testing of Mechanical and Surface Properties of Thin Films"; pp. 325–56 in *Comprehensive Structural Integrity*, Vol. 8, Edited by W. Gerberich and W. Yang. Elsevier, Oxford, 2003.

[10]H. Kahn, R. Ballarini, and A. H. Heuer, "Mechanical Fatigue of Polysilicon: Effects of Mean Stress and Stress Amplitude," *Acta Mater.* **54** [4] 667–78 (2006).

[11]K. E. Petersen, "Silicon as a Mechanical Material," *Proc. IEEE* **70**, 420–57 (1982).

[12]T. Tsuchiya, O. Tabata, J. Sakata, and Y. Taga, "Tensile Testing of Polycrystalline Silicon Thin Films Using Electrostatic Force Grip," *Trans. Int. Elect. Engineers Jpn.*, **116-E** [10] 441–446 (1996).

[13]T. Tsuchiya, O. Tabata, J. Sakata, and Y. Taga, "Specimen Size Effect on Tensile Strength of Surface-Micromachined Polycrystalline Silicon Thin Films," *J. Microelectromech. Syst.*, **7**, 106–13 (1998).

[14]B. L. Boyce, J. M. Grazier, T. E. Buchheit, and M. J. Shaw, "Strength Distributions in Polycrystalline Silicon MEMS," *J. Microelectromech. Syst.* **16** [2] 179–90 (2007).

[15]T. Tsuchiya, "Tensile Testing of Silicon Thin films," *Fatigue Fracture Eng. Materi. Struct.* **28**, 665–74 (2005).

[16]W. N. Sharpe, O. Jadaan, G. M. Beheim, G. D. Quinn, and N. N. Nemeth, "Fracture Strength of Silicon Carbide Microspecimens," *J. Microelectromech. Syst.*, **14** [5] 903–13 (2005).

[17]A. McCarty and I. Chasiotis, "Description of Brittle Failure of Non-Uniform MEMS Geometries," *Thin Solid Films*, **515** [6] 3267–76 (2007).

[18]S. D. Pang, Z. P. Bažant, and J.-L. Le, "Statistics of Strength of Ceramics: Finite Weakest Link Model and Necessity of Zero Threshold," *Int. J. Frac.*, **154**, 131–45 (2008).

[19]J.-L. Le, Z. P. Bažant, and M. Z. Bazant, "Unified Nano-Mechanics Based Probabilistic Theory of Quasibrittle and Brittle Structures: I. Strength, Crack Growth, Lifetime and Scaling," *J. Mech. Phys. Solids*, **59**, 1291–321 (2011).

[20]W. Weibull, "The Phenomenon of Rupture in Solids"; pp. 1–55 in *Proceedings of Royal Swedish Institute of Engineering Research*, Vol. 153. Stockholm, 1939.

[21]W. Weibull, "A Statistical Distribution Function of Wide Applicability," *J. Appl. Mech. ASME*, **153** [18] 293–7 (1951).

[22]Z. P. Bažant and J. Planas, *Fracture and Size Effect in Concrete and Other Quasibrittle Materials*. CRC Press, Boca Raton and London, 1998.

[23]D. Munz and T. Fett, *Ceramics: Mechanical Properties, Failure Behavior, Materials Selection*. Springer-Verlag, Berlin, 1999.

[24]R. M. Christensen, *The Theory of Material Failure*. Oxford University Press, Oxford, 2013.

[25]R. A. Fisher and L. H. C. Tippett, "Limiting Forms of the Frequency Distribution of the Largest and Smallest Member of a Sample," *Proc. Cambridge Philos. Soc.*, **24**, 180–90 (1928).

[26]M. Z. Bazant, "The Largest Cluster in Subcritical Percolation," *Phys. Rev. E*, **62**, 1660–9 (2000).

[27]M. Z. Bazant, "Stochastic Renormalization Group in Percolation," *Physica A*, **316**, 451–77 (2002).

[28]R. van der Hofstad and F. Redig, "Maximal Clusters in Non-Critical Percolation and Related Models," *J. Statist. Phys.*, **122** [4] 671–703 (2006).

[29]Z. P. Bažant, J.-L. Le, and M. Z. Bazant, "Scaling of Strength and Lifetime Distributions of quaSibrittle Structures Based on Atomistic Fracture Mechanics," *Proc. Nat'l. Acad. Sci., USA*, **106** [28] 11484–9 (2009).

[30]E. D. Reedy, "Singular Stress Fields at the Intersection of a Grain Boundary and a Stress-Free Edge in a Columnar Polycrystal," *J. Appl. Mech.*, **78**, 014502, 4pp (2011).

[31]K. Yasutake, M. Iwata, K. Yoshii, M. Umeno, and H. Kawabe, "Crack Healing and Fracture Strength of Silicon Crystals," *J. Mater. Sci.*, **21** [6] 2185–92 (1986).

[32]Z.P. Bažant and S.-D. Pang, "Mechanics Based Statistics of Failure Risk of Quasibrittle Structures and Size Effect on Safety Factors," *Proc. Nat'l. Acad. Sci., USA* **103** [25] 9434–9 (2006).

[33]Z. P. Bažant and S. D. Pang, "Activation Energy Based Extreme Value Statistics and Size Effect in Brittle and Quasibrittle Fracture," *J. Mech. Phys. Solids*, **55**, 91–134 (2007).

[34]P. Grassl and Z. P. Bažant, "Random Lattice-Particle Simulation of Statistical Size Effect in Quasi-Brittle Structures Failing at Crack Initiation," *J. Eng. Mech. ASCE*, **135** [2] 85–92 (2009).

[35]S. S. Hazra, M. S. Baker, J. L. Beuth, and M. P. de Boer, "Demonstration of an In-Situ on-Chip Tester," *J. Micromech. Microeng.*, **19** [8] 082001, 5pp (2009).

[36]B. L. Boyce, "A Sequential Tensile Method for Rapid Characterization of Extreme-Value Behavior in Micro Fabricated Materials," *Exp. Mech.*, **50**, 993–7 (2010).

[37]S. M. -M. Dubois, G. -M. Rignanese, T. Pardoen, and J.-C. Charlier, "Ideal Strength of Silicon: An *Ab Initio* Study," *Phy. Rev. B.*, **74**, 235203, 7pp (2006).

[38]A. Cannone Falchetto, J.-L. Le, M. I. Turos, and M. O. Marasteanu, "Indirect Determination of Size Effect on Strength of Asphalt Mixture at Low Temperatures," *Mater. Struc.*, **47** [1–2] 157–69 (2014).

[39]J.-L. Le and Z. P. Bažant, "Scaling of Static Fracture of Quasibrittle Structures: Strength, Lifetime and Fracture Kinetics," *J. Appl. Mech.*, **79**, 031006, 10pp (2012).

[40]J.-L. Le, A. Cannone Falchetto, and M. O. Marasteanu, "Determination of Strength Distribution of Quasibrittle Structures from Size Effect Analysis," *Mech. Mater.*, **66**, 79–87 (2013).

[41]Z. P. Bažant, "Scaling Theory of Quaisbrittle Structural Failure," *Proc. Nat'l. Acad. Sci., USA*, **101** [37] 13400–7 (2004).

[42]Z. P. Bažant, *Scaling of Structural Strength*, 2nd edition. Elsevier, London, 2005. □

Jia-Liang Le: Jia-Liang Le is currently an assistant professor in the Department of Civil, Environmental and Geo- Engineering at the University of Minnesota. He received his Bachelor of Engineering (First Class Honors) in Civil Engineering from the National University of Singapore (NUS) in 2003, a Master of Engineering from NUS in 2005, and a Ph.D. in Structural Mechanics from Northwestern University in 2010. His research interests include probabilistic mechanics, fracture mechanics, scaling, reliability analysis and computational mechanics. The current research is focused on quasibrittle materials and structures at various scales, ranging from microelectromechanical systems to large-scale civil infrastructure. He received the Walter P. Murphy Fellowship and Royal Cabell Fellowship from Northwestern University, the Undergraduate Faculty Award from the University of Minnesota, and the 2014 Best Paper Award from the American Association of Rock Mechanics.

Roberto Ballarini: Roberto Ballarini is Thomas and Laura Hsu Professor and Chair of the Department of Civil and Environmental Engineering at University of Houston. He joined the University of Houston after having served for eight years as James Record Chair at University of Minnesota and for twenty year as Leonard Case Professor of Engineering at Case Western Reserve University. Ballarini's multidisciplinary research focuses on the development and application of theoretical and experimental techniques to characterize the response of materials to mechanical, thermal, and environmental loads. He is particularly interested in formulating analytical and computational models for characterizing fatigue and fracture of materials and structures. His research, which has been applied to problems arising in civil engineering, mechanical and aerospace engineering, materials science, electromechanical systems, biological tissues and prosthetic design, has been featured in the popular press, including the New York Times Science Times, American Scientis, Geo and Pour La Science. His current research involves theoretical, computational and experimental studies of microelectromechanical systems (MEMS) and nanoscale biological and synthetic materials, bioinspired design of composite structures and materials, seismic-resistant structural steel systems, size effects in quasibrittle materials and structures, and the collapse of the I-35W Bridge in Minneapolis.

Zhiren Zhu: Zhiren Zhu is currently a M.S. candidate in the Department of Civil, Environmental, and Geo-Engineering at the University of Minnesota. He received the B.S. degree in Civil Engineering from the University of Massachusetts, Amherst in 2009.